Experimental study of transient coupling of PVC formation and flame shape transition in a bi-stable turbulent swirl flame

M. Stöhr*[,1], K. Oberleithner[2], C. M. Arndt[1], A. M. Steinberg[1,3] and W. Meier[1]

[1] Institute of Combustion Technology, German Aerospace Center (DLR), 70569 Stuttgart, Germany
[2] Institut für Strömungsmechanik und Technische Akustik, HFI, Müller-Breslau Straße 8, 10623 Berlin, Germany
[3] Present address: Institute for Aerospace Studies, Univ. of Toronto, 4925 Dufferin St., Toronto, Canada M3H 5T6

Abstract

The dynamics of a bi-stable swirl flame in a gas turbine model combustor is studied using simultaneous PIV and OH-PLIF at 10 kHz. For most operating conditions, the flames in the combustor either feature a steady V-shape or a steady M-shape. A hydrodynamic instability in the form of the so-called precessing vortex core (PVC) occurs only for the M-shaped flames. For the V-flames, the PVC is suppressed due to radial density gradients at the burner nozzle as shown in an accompanying study (Oberleithner et al., Proc 7th Euro Comb Meeting 2015). At some intermediate operating conditions, bi-stable flames occur where the flame alternates randomly between V- and M-shape. This work investigates a transition from V- to M-shape, focusing on the implied transient formation of a PVC and its role in the transition of flame type. The measurements reveal a sequence of events where the PVC forms *before* the transition of the flame shape. The sequence starts with a slight lift of the flame root due to a random turbulent event, which induces a density profile that is favorable for formation of the PVC. The subsequently forming PVC creates an unsteady lower stagnation point that causes a lift-off of the flame root, which finally results in the formation of a detached M-shaped flame.

Introduction

The stabilization of highly turbulent flames in modern gas turbine (GT) combustors is commonly achieved by imposing a swirling motion on the reactants. The resulting vortex breakdown of the swirling flow in the combustion chamber implies the formation of an inner recirculation zone (IRZ), where hot burned gas is transported back to the inlet where it mixes with the unburned reactants. This enhances ignition of the unburned gas and thus helps to operate the flames under the required fuel-lean and high-velocity conditions. The formation of the IRZ is often (but not always) accompanied by the occurrence of coherent flow structures such as the precessing vortex core (PVC). The formation of the PVC involves the occurence of a helical vortex in the shear layer of the IRZ [1]. Both experimental and numerical studies have shown that this vortex can lead to enhanced mixing of fuel and air [2, 3, 4, 5] or burned and unburned gas [6, 7] and may cause roll-up, stretch or local quenching of reaction zones [7, 8].

For some combustors, it has been reported that PVCs are encountered for all reacting conditions [9, 10, 11, 7]. For other combustors, however, it is suppressed for certain, but not necessarily all reacting cases [12, 13, 14, 15, 16]. The suppression can be triggered by changes of steam content and preheat temperature [17], swirl number [18], thermal power [19], pilot flow rate [20], or axial air injection [21]. In addition, bi-stable operating conditions were encountered where the flame changes intermittently between different states with and without PVC [22]. The appearance or disappearance of a PVC is usually accompanied by a major change of flame shape [18, 22], which in turn affects the combustor performance in terms of thermoacoustics, NOx emissions, flashback or blowout. Given the strong effects of the PVC on the flame mentioned above, it is desirable to better understand the mechanisms of the observed formation and suppression of PVCs in swirl combustors.

In an accompanying study [23], Oberleithner et al. examine the time-averaged flow in a swirl combustor using linear stability analysis (LSA) of two reacting cases, one featuring an M-shaped flame with PVC and the other a V-shaped flame without PVC. Based on the velocity and density field, the LSA provides growth rate and frequency of a possible hydrodynamic instability. For one case where a PVC appeared in the experiment, the analysis shows a global instability that manifests in a single-helical mode with its wavemaker located at the combustor inlet. The frequency of the global mode is in excellent agreement with the measured oscillation frequency and the growth rate is approximately zero, indicating the marginally stable limit-cycle. For the attached V-flame without PVC, strong radial density/temperature gradients are encountered at the inlet, which are shown to suppress the global instability. The results indicate that it is mainly the density field, which in turn depends on the location and shape of the flame, that determines whether a PVC forms or not.

Between the two conditions with and without PVC, the experiments reveal a bi-stable condition where the flame alternates randomly between V- and M-shape. This implies that a PVC is repeatedly formed and suppressed, and therefore the bi-stable case allows studying the transient formation of a PVC and its role in the transition of

*Corresponding author: michael.stoehr@dlr.de

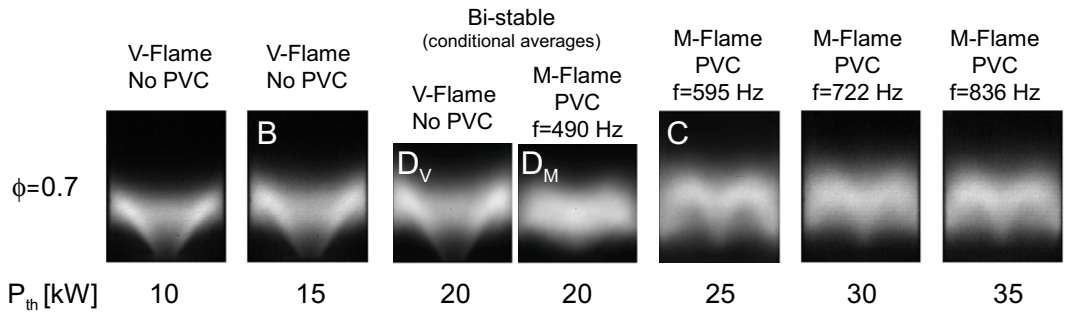

Figure 1: Flame shapes for different values of thermal power $P_{\rm th}$ at an equivalence ratio of ϕ=0.7.

flame type. The results might be relevant to other swirl combustors where bi-stable flames have been reported [24, 25, 26, 27, 22]. A particular question is whether the flame form first changes and then the PVC is formed, or if at first the PVC forms and this then triggers the change of flame shape. The aim of this work is to study the dynamics and causality of a transition event at the bi-stable condition using time-resolved, simultaneous particle image velocimetry (PIV) and OH planar laser-induced fluorescence (PLIF). The different temporal evolutions of flame shape transition and PVC formation are evaluated based on a set of specific parameters extracted from the time-resolved data. The critical steps of the transition are analyzed in more detail based on image sequences of velocity and OH, and interpreted using the results of the LSA in the accompanying study Ref. [23].

Combustor and diagnostic setup

The combustor and the diagnostic setup used in this work are equivalent to those used in a previous work by Steinberg et al. [19]. A brief description is provided below.

Measurements were performed in a GT-typical swirl combustor derived from an industrial design by Turbomeca, which is operated in perfectly premixed mode with methane and air at atmospheric pressure. The reactants first enter a plenum and then pass through a swirl generator with 12 radial vanes. The swirling flow then enters the combustor chamber through a burner nozzle with diameter D=27.85mm and a conical inner bluff body. The chamber has a square cross-section of 85×85 mm^2 and a height of 114 mm. Optical access to the chamber is provided by side walls made of quartz glass held by metal posts in the corners. The exit is composed of a conical part followed by an exhaust duct with 40 mm inner diameter.

Simultaneous OH-PLIF, OH-chemiluminescence (CL) and stereoscopic PIV were performed at a repetition rate of 10 kHz. Due to limitations of laser pulse energy and camera resolution, the PIV field of view was reduced to 49 mm $\times$ 38 mm. The OH-PLIF was excited at 283.2 nm by a frequency-doubled dye laser (Sirah Credo), pumped by a Nd:YAG diode-pumped solid state (DPSS) laser (Edgewave IS8IIE). The PLIF signal was collected with an intensified high-speed CMOS camera (LaVision HSS 5 with LaVision HS-IRO) equipped with a fast UV lens (Cerco, f=45mm, f/1.8) and a bandpass filter (300-325 nm). A second, identical camera/lens/filter arrangement was used for OH-CL imaging. The stereo-PIV system consisted of a dual-cavity Nd:YAG DPSS laser (Edgewave IS6II-DE) with a pulse energy of 2.6 mJ/pulse at 532 nm. TiO_2 particles with diameter 1 μm were used as flow tracers. Particle images were recorded with a pair of high-speed CMOS cameras (LaVision HSS 8), equipped with commercial camera lenses (Tokina, f=100 mm, set to f/5.6). Vector fields were computed from the particle images using a commercial PIV software (LaVision DaVis 8.0) with a multi-scale cross-correlation algorithm.

Characteristics of the bi-stable flame

Bi-stable flames are encountered at operating conditions between the two ranges of conditions where stable V-flames and stable M-flames occur. For an equivalence ratio of ϕ=0.7, the transition of flame states can be seen in the OH-CL images shown in Fig. 1. At a thermal power of P=10 and 15 kW, the flames are attached at the nozzle exit (bottom of the image) and exhibit a stable V-shape, whereas for P=25, 30 and 35 kW, a lifted M-shaped flame is found. The analysis in the accompanying work [23] shows that the M-flames always exhibit a PVC, while for V-flames generally no PVC occurs. The suppression of the PVC at P=15 kW and its formation at P=25 kW are further examined in Ref. [23] (where these cases are labeled B and C, respectively) using LSA, showing that for the V-flames the suppression is caused by radial density gradients near the burner nozzle exit.

For an intermediate thermal power of P=20 kW, the flame is bi-stable, i.e., it alternates about once per second between an attached V-shaped form without PVC, and a detached M-shaped form with PVC. The two respective conditional averages of OH-CL shown in Fig. 1 were determined using the simultaneously measured OH-PLIF signal near the nozzle (see next section) to distinguish between the attached and detached flame form. In remainder of this work the temporal evolution and causality of a transition from V- to M-form, during which the formation of the PVC is initiated, is analyzed.

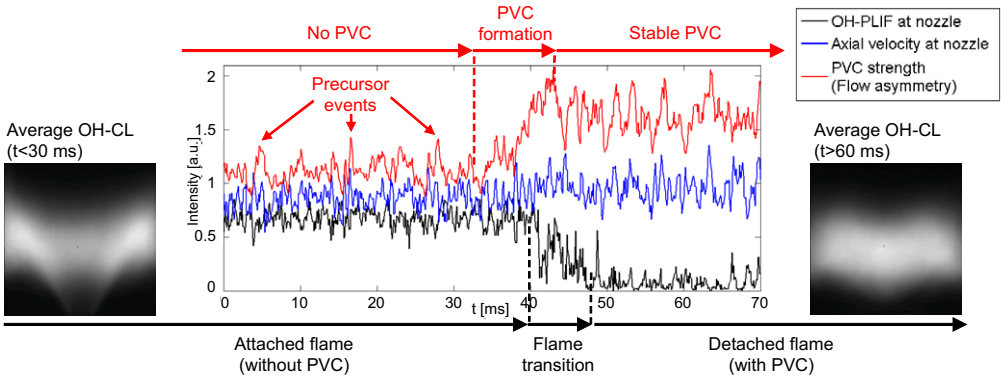

Figure 3: Temporal evolution of flow asymmetry (red), axial inflow velocity (blue) and OH-PLIF signal at the nozzle (black) during the transition from a V-shaped flame to an M-shaped flame.

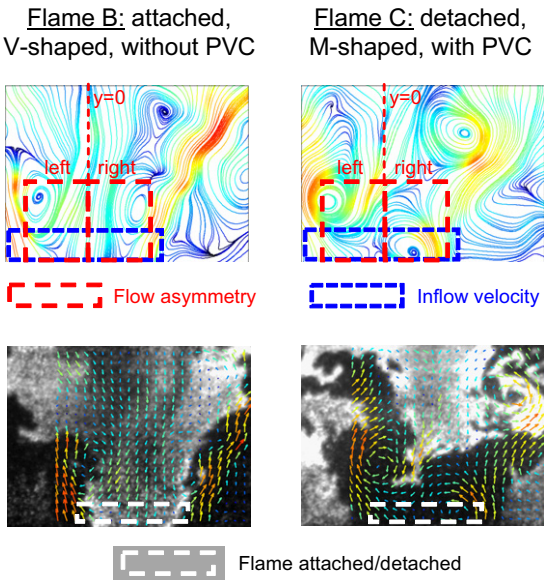

Figure 2: Selected regions for the determination of flow asymmetry (red), axial inflow velocity (blue) and OH-PLIF signal at the nozzle (white).

Transition from V- to M-flame

The analysis of the transition is based on three quantities, which are estimated from the measured fields of velocity and OH. Exemplary instantaneous measurements of flow field and OH-PLIF for a V-flame (case B) and an M-flame (case C) are shown in Fig. 2. The grayscale OH-PLIF images can be interpreted as follows: Regions without OH (black) represent gas with low or medium temperature (T<1500 K), i.e., unburned gas possibly mixed with adjacent burned gas. High levels of OH (light gray to white) indicate superequilibrium OH, which is formed in the reaction zones and has a half-life period of ≈1 ms under atmospheric pressure conditions [28]. Regions with medium and low levels of OH (medium and dark gray) represent burned gas where the OH concentration has decayed toward equilibrium while it was transported away from the reaction zone.

The first quantity $a(t)$ is the asymmetry of the flow field above the nozzle (marked red). It is a measure of the presence and strength of the PVC. The asymmetry $a(t)$ is calculated as the squared difference between the left and right half of the flow field, i.e., $a(t) = \sum_{x,y} |\mathbf{u}(x,y,t) - \mathbf{u}(x,-y,t)|^2$ (the elements of $\mathbf{u} = (u_x, u_r, u_\theta)^T$ are the axial, radial, and azimuthal velocity components, respectively). The value of $a(t)$ is low for the symmetric flow without PVC and high when the asymmetric vortex pattern of the PVC appears. The second quantity $b(t)$ is the OH-PLIF signal in the zone directly above the nozzle (marked white). It is calculated as the sum of counts g in this region of the OH-PLIF image, i.e., $b(t) = \sum_{x,y} g(x,y,t)$. Values of $b(t)$ are high when the flame is attached and low when it is detached. The third quantity $c(t)$ is the flow velocity into the combustion chamber, taken over the region above the nozzle (marked blue), i.e., $c(t) = \sum_{x,y} u_x(x,y,t)$. While the temporal average of $c(t)$ is similar for both flame forms, temporary fluctuations might influence the transition. In the following discussion, for all three quantities only relative changes are considered, and therefore they will be plotted in arbitrary units (a.u.).

Figure 3 shows the dynamics of the three quantities during a transition from V-shape to M-shape. For t<30 ms, the V-flame remains largely stable. Then, starting at t≈32 ms, the asymmetry (red) increases indicating the formation of the PVC. The flame remains attached until t≈40 ms as indicated by the OH signal at the nozzle (black). For t>50 ms, a detached, M-shaped flame with PVC has stabilized. The temporal dynamics show that at first the PVC is formed, and then the attached flame lifts and changes its shape. Prior to the transition, three precursor events at t≈5, 17 and 28 ms can be observed where a PVC starts to form, but is quickly suppressed again. The cause for the onset of the PVC oscillations remains unclear at first and thus requires a more detailed investigation of the PIV and OH-PLIF image sequences. In the following, we first focus on a precursor event and thereafter on the transition.

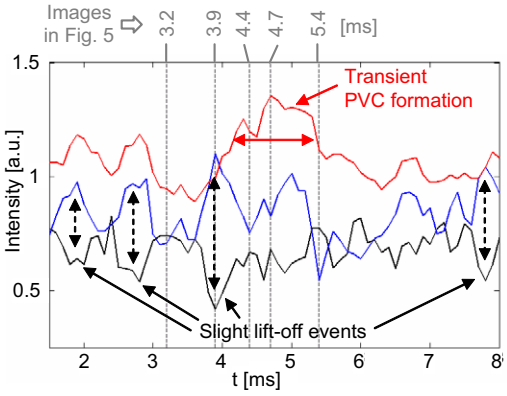

Figure 4: Temporal evolution of flow asymmetry (red), axial inflow velocity (blue) and OH-PLIF signal at the nozzle (black) during the precursor event around t=5 ms.

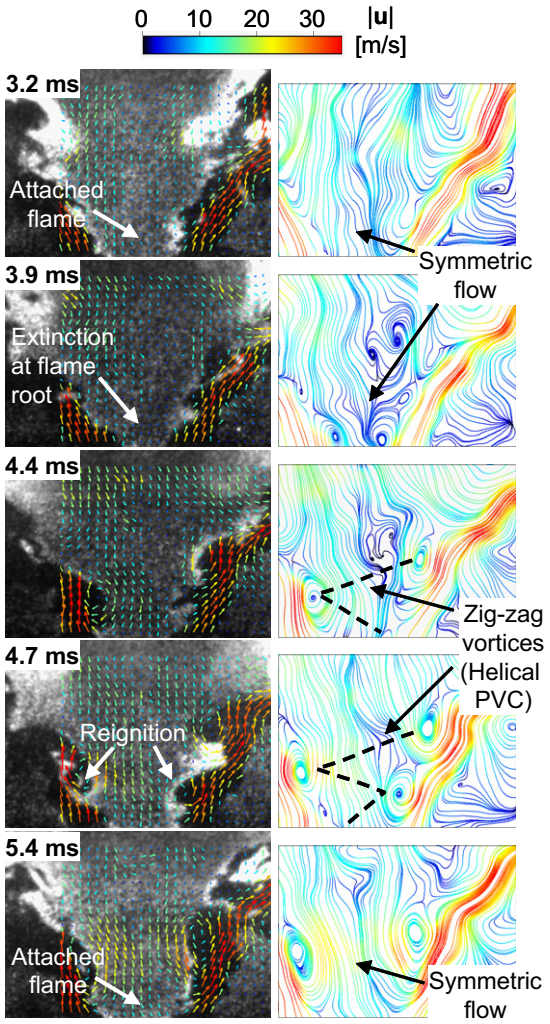

Figure 5: Time-resolved PIV and OH-PLIF measurement during the precursor event around t=5 ms. The PIV particle density images are used as an approximate marker of gas density.

Precursor event

The dynamics of the precursor event at around t=5 ms is plotted in more detail in Fig. 4. It shows that the inflow velocity (blue) fluctuates randomly, and that these fluctuations correlate oppositely with the OH at the nozzle (black). This is expected since the inflowing unburned gas contains no OH. The random nature of the inflow fluctuations suggests that these are caused by turbulent motion of the unburned inflow.

The corresponding image sequence in Fig. 5 shows that at t=3.2 ms, the flow field is largely symmetric without PVC and the flame is attached. At t=3.9 ms, the increased inflow leads to quenching of the flame root at the bottom and to an increased amount of unburned gas near the nozzle. The analysis in Ref. [23] has shown that the presence of unburned gas above the nozzle forms a density field that favors the formation of a PVC. Indeed, it is seen that at t=4.4 and 4.7 ms, a PVC has formed. The flame root, however, re-ignites at t=4.7 ms and therefore the region of unburned gas is reduced again. At t=5.4 ms, a larger zone of burned gas above the nozzle has re-established and the PVC has disappeared.

Dynamics of flame transition

The dynamics of the flame transition and PVC formation from t=34 to t=48 ms is plotted in Fig. 6 and the corresponding image sequence is shown in Fig. 7. Until t=37.7 ms, the flame is attached and the flow does not exhibit a PVC. At t=38.1 ms, an increased inflow occurs like at the onset of the precursor event (t=3.9 ms) described above. The higher inflow again causes quenching at the flame root and an increased amount of unburned gas near the nozzle. Like in the precursor event, the increased density of unburned gas near the nozzle is followed by the formation of a PVC at t=38.5 ms. Other than in the precursor event, however, the PVC now persists slightly longer. Apparently, at this stage the PVC is at the border of stability, and the decision whether it persists or disappears again depends on small local variations of the density and flow fields.

During its initial formation at t=38.5 and 40.1 ms, the PVC exhibits the typical zig-zag vortex pattern, but no stagnation point has yet appeared and therefore the flame is still attached. As described in Ref. [7], the unsteady lower stagnation point is an important feature of the PVC as it determines the position of the flame root. Starting at t=41.2 ms, an unsteady stagnation point appears and accordingly, the flame root detaches and lifts off. This further enlarges the region of unburned gas above the nozzle, and presumably further supports the PVC formation until it is fully established at $t\approx$48 ms.

In conclusion, it is certainly difficult to fully characterize the transition mechanism, since this would require 3D time-resolved measurements. Nevertheless, the planar high-speed measurements in combination with the stability analysis of the steady states B and C in Ref. [23] suggest the following sequence of events and their causality: Starting point is a sufficiently strong increase of inflow rate, probably caused by random turbulence. This leads to local extinction at the flame root and, due to the

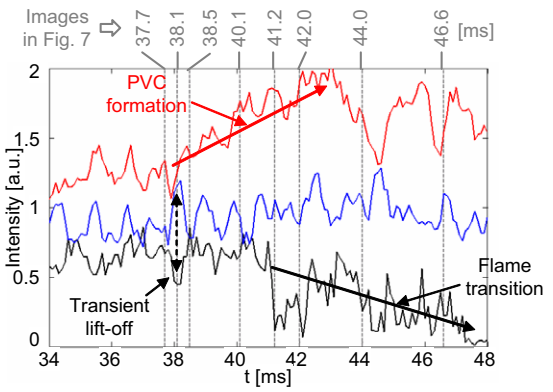

Figure 6: Temporal evolution of flow asymmetry (red), axial inflow velocity (blue) and OH-PLIF signal at the nozzle (black) during the transition event.

resulting favorable changes of density, initiates the formation of a PVC. In many cases like the precursor events, the favorable density profile remains only for a short time, and thus the PVC is suppressed again and the flame remains in V-shape. In some cases, however, the PVC establishes slightly further such that an unsteady stagnation point is formed. It is seen that this point induces a lift-off of the flame, which in turn enlarges the region of unburned gas near the nozzle that further supports the PVC. In addition, it is likely that the PVC causes additional mixing in the IRZ [29] and flattens the radial density gradient, which in turn further promotes the formation of the PVC. Subsequently the PVC is fully established and the flame further lifts off and approaches the detached M-shape.

Summary and Conclusions

The present work investigates a bi-stable turbulent swirl flame that alternates randomly between a V-shape without PVC and an M-shape with PVC. By means of time-resolved PIV and OH-PLIF measurements, flame structure and flow field are monitored during a transition from V- to M-shape, which implies a transient formation of the PVC. The measurements reveal a sequence of events where the PVC forms *before* the transition of the flame shape. The sequence starts with a slight lift of the flame root due to a random turbulent event, which induces a density profile that, according to the LSA of the reacting cases, is favorable for formation of the PVC. The PVC creates an unsteady lower stagnation point that causes a lift-off of the flame root, which finally results in the formation of a detached M-shaped flame.

The results highlight the complex interplay of flow/density field, unsteady coherent vortices and flame propagation that determines the stabilization of turbulent swirl flames: The stability analysis of the time-averaged flow in the accompanying study [23] successfully identified the PVC as a global hydrodynamic instability and demonstrated the importance of the fluid density distrbution near the burner nozzle. The present time-resolved

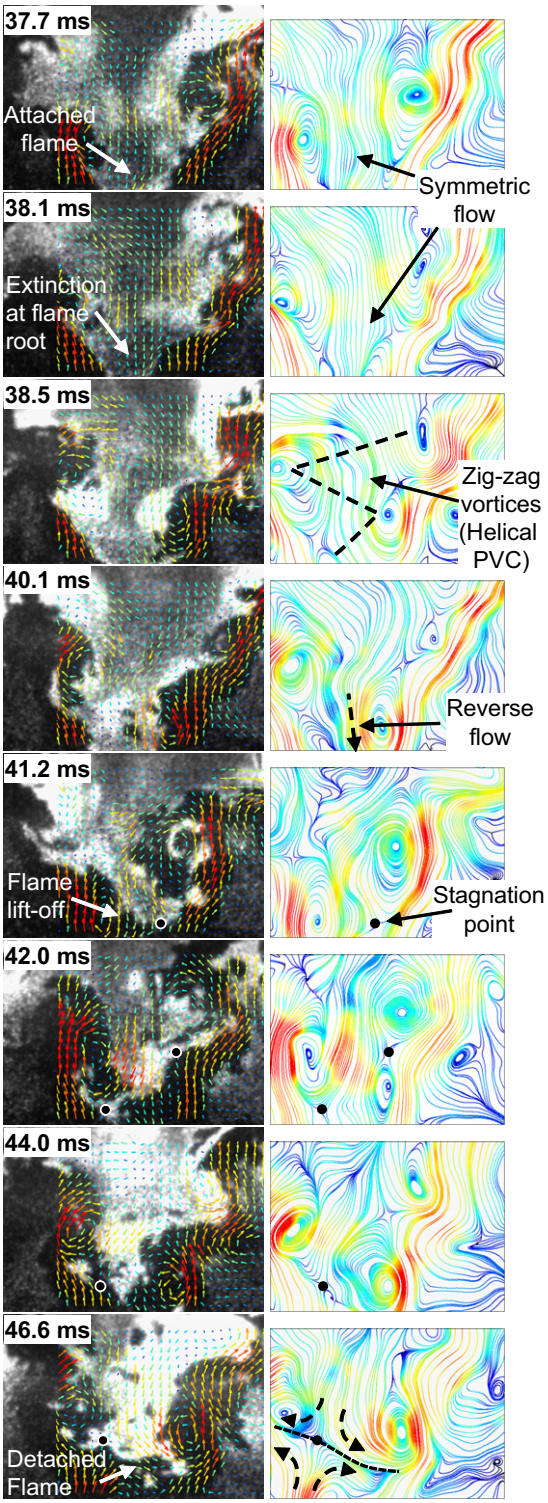

Figure 7: Time-resolved PIV and OH-PLIF measurement during the transition event. The velocity color scale is the same as in Fig. 5.

measurements reveal that the PVC induces an unsteady lower stagnation point, which, at certain critical conditions like the present bi-stable case, causes the lift-off of an otherwise attached flame. A change of flame shape, in turn, causes a change of the flow and density field near

the burner nozzle. Given the essential role of the PVC in this interplay, the analysis of the hydrodynamic stability of the reacting swirling flow is a critical step in the design of a swirl combustor.

References

[1] N. Syred, Prog. Energy Combust. Sci. 32 (2006) 93 – 161.

[2] M. Freitag, K. M., M. Gregor, D. Geyer, C. Schneider, A. Dreizler, J. Janicka, Int. J. Heat Fluid Flow 27 (2006) 636–643.

[3] J. Fröhlich, M. Garcia-Villalba, W. Rodi, Flow Turbul. Comb. 80 (2008) 47–59.

[4] D. Galley, S. Ducruix, F. Lacas, D. Veynante, Combust. Flame 158 (2011) 155–171.

[5] M. Stöhr, C. Arndt, W. Meier, Proc. Combust. Inst. 35 (2015) 3327–3335.

[6] M. Stöhr, R. Sadanandan, W. Meier, Exp. Fluids 51 (2011) 1153–1167.

[7] M. Stöhr, I. Boxx, C. D. Carter, W. Meier, Combust. Flame 159 (2012) 2636–2649.

[8] M. Stöhr, C. Arndt, W. Meier, Proc. Combust. Inst. 34 (2013) 3107–3115.

[9] P. M. Anacleto, E. C. Fernandes, M. V. Heitor, S. I. Shtork, Combust. Sci. Technol. 175 (2003) 1369–1388.

[10] N. Patel, S. Menon, Combust. Flame 153 (2008) 228–257.

[11] P. Fokaides, M. Wei, M. Kern, N. Zarzalis, Flow Turbul. Comb. 83 (2009) 511–533.

[12] L. Selle, G. Lartigue, T. Poinsot, R. Koch, K.-U. Schildmacher, W. Krebs, B. Prade, P. Kaufmann, D. Veynante, Combust. Flame 137 (2004) 489–505.

[13] C. Schneider, A. Dreizler, J. Janicka, Flow Turbul. Comb. 74 (2005) 103–127.

[14] K.-U. Schildmacher, R. Koch, H.-J. Bauer, Flow Turbul. Comb. 76 (2006) 177–197.

[15] M. Freitag, J. Janicka, Proc. Combust. Inst. 31 (2007) 1477–1485.

[16] A. De, S. Zhu, S. Acharya, J. Eng. Gas Turb. Power 132 (2010) 071503.

[17] S. Terhaar, K. Oberleithner, C. O. Paschereit, Combust. Sci. Technol. 186 (2014).

[18] C. Duwig, L. Fuchs, Phys. Fluids 19 (2007) 5103.

[19] A. M. Steinberg, C. M. Arndt, W. Meier, Proc. Combust. Inst. 34 (2013) 3117–3125.

[20] A. X. Sengissen, A. V. Giauque, G. S. Staffelbach, M. Porta, W. Krebs, P. Kaufmann, T. J. Poinsot, Proc. Combust. Inst. 31 (2007) 1729–1736.

[21] S. Terhaar, T. G. Reichel, C. Schrödinger, L. Rukes, C. O. Paschereit, K. Oberleithner, J Propul Power 31 (2014) 219–229.

[22] S. Hermeth, G. Staffelbach, L. Y. M. Gicquel, V. Anisimov, C. Cirigliano, T. Poinsot, Combust. Flame 161 (2014) 184–196.

[23] K. Oberleithner, M. Stöhr, S. H. Im, C. O. Paschereit, in: Proceedings of the 7th European Combustion Meeting (2015) Budapest, Hungary.

[24] W. Polifke, A. Fischer, T. Sattelmayer, J. Eng. Gas Turb. Power 125 (2003) 20–27.

[25] D. Fritsche, M. Furi, K. Boulouchos, Combust. Flame 151 (2007) 29–36.

[26] F. Biagioli, F. Güthe, B. Schuermans, Exp. Therm. Fluid Sci. 32 (2008) 1344–1353.

[27] T. F. Guiberti, D. Durox, P. Scouflaire, T. Schuller, F. Biagioli, F. Güthe, B. Schuermans, Proc. Combust. Inst. 35 (2015) 1385–1392.

[28] R. Sadanandan, M. Stöhr, W. Meier, Appl. Phys. B 90 (2008) 609–618.

[29] S. Terhaar, O. Krüger, C. O. Paschereit, Journal of Engineering for Gas Turbines and Power 137 (2015) 041503.